REPORT DOCUMENTATION PAGE

Form Approved OMB NO. 0704-0188

1. REPORT DATE (DD-MM-YYYY)	2. REPORT TYPE	3. DATES COVERED (From - To)
13-04-2017	Final Report	15-Jul-2015 - 14-Jan-2017

4. TITLE AND SUBTITLE

Final Report: Instrument Development for a Long-Range, High-Resolution 3D Imaging Photon Counting LADAR

5a. CONTRACT NUMBER
W911NF-15-1-0363

5b. GRANT NUMBER

5c. PROGRAM ELEMENT NUMBER
611103

6. AUTHORS

Renu Tripathi, Gour S. Pati

5d. PROJECT NUMBER

5e. TASK NUMBER

5f. WORK UNIT NUMBER

7. PERFORMING ORGANIZATION NAMES AND ADDRESSES

Delaware State University
1200 N. Dupont Highway

Dover, DE 19901 -2277

8. PERFORMING ORGANIZATION REPORT NUMBER

9. SPONSORING/MONITORING AGENCY NAME(S) AND ADDRESS (ES)

U.S. Army Research Office
P.O. Box 12211
Research Triangle Park, NC 27709-2211

10. SPONSOR/MONITOR'S ACRONYM(S)
ARO

11. SPONSOR/MONITOR'S REPORT NUMBER(S)
66892-CH-RIP.2

12. DISTRIBUTION AVAILIBILITY STATEMENT

Approved for Public Release; Distribution Unlimited

13. SUPPLEMENTARY NOTES

The views, opinions and/or findings contained in this report are those of the author(s) and should not contrued as an official Department of the Army position, policy or decision, unless so designated by other documentation.

14. ABSTRACT

We proposed to develop a high-resolution three-dimensional imaging LADAR system based on the principle of photon-counting and highly-resolution time-correlated measurements. Imaging capability of this photon-counting LADAR (PC-LADAR) was also proposed to be enhanced using polarimetric measurements. Following are some of our notable accomplishments:

1. Components for developing the PC-LADAR system have been acquired. This includes purchasing of major components such as picosecond laser sources (LDH-P-C-705 and LDH-P-C-840, PicoQuant), single photon

15. SUBJECT TERMS

Lidar, photon counting detector, pulsed laser, time correlated photon counting, remote sensing

16. SECURITY CLASSIFICATION OF:			17. LIMITATION OF ABSTRACT	15. NUMBER OF PAGES	19a. NAME OF RESPONSIBLE PERSON
a. REPORT	b. ABSTRACT	c. THIS PAGE			Renu Tripathi
UU	UU	UU	UU		19b. TELEPHONE NUMBER: 302-857-6298

Report Title

Final Report: Instrument Development for a Long-Range, High-Resolution 3D Imaging Photon Counting LADAR

ABSTRACT

We proposed to develop a high-resolution three-dimensional imaging LADAR system based on the principle of photon-counting and highly-resolution time-correlated measurements. Imaging capability of this photon-counting LADAR (PC-LADAR) was also proposed to be enhanced using polarimetric measurements. Following are some of our notable accomplishments:

1. Components for developing the PC-LADAR system have been acquired. This includes purchasing of major components such as picosecond laser sources (LDH-P-C-705 and LDH-P-C-840, PicoQuant), single photon detectors (PD-100-CTC-FC, Micro Photon Devices and SPCM-AQRH-16, Pacer-usa), picosecond event-timer (HydraHarp 400, PicoQuant), and high-bandwidth oscilloscope (DSO-X-4054A, Keysight Technologies) etc.
2. A software interface for PC-LADAR is developed for performing synchronized beam scanning with the laser transmitter.
3. Receiver assembly for PC-LADAR is designed using a large aperture (eight inch) telescope objective lens. Assembly design for the complete system is currently under progress.
4. Basic characterizations of the event-timer module for time-of-flight (TOF) measurements have been performed.
5. Experiments using a scanning LADAR prototype were conducted to demonstrate improvement in TOF (or range) resolution using a new multi-pulse detection scheme.
6. Students (one graduate student and two undergraduate students) are trained in performing LADAR system design, hardware testing and data acquisition.

Enter List of papers submitted or published that acknowledge ARO support from the start of the project to the date of this printing. List the papers, including journal references, in the following categories:

(a) Papers published in peer-reviewed journals (N/A for none)

Received		Paper
04/13/2017	1	Zachary Warren, Selim M. Shahriar, Renu Tripathi, Gour S. Pati. Experimental and Theoretical Comparison of Different Optical Excitation Schemes for a Compact Coherent Population Trapping Rb Vapor Clock, Metrologia, ( ): . doi:
		1,039,092.00
TOTAL:	**1**	

Number of Papers published in peer-reviewed journals:

(b) Papers published in non-peer-reviewed journals (N/A for none)

Received		Paper
TOTAL:		

Number of Papers published in non peer-reviewed journals:

(c) Presentations

Number of Presentations: 0.00

Non Peer-Reviewed Conference Proceeding publications (other than abstracts):

Received	Paper

TOTAL:

Number of Non Peer-Reviewed Conference Proceeding publications (other than abstracts):

Peer-Reviewed Conference Proceeding publications (other than abstracts):

Received	Paper

TOTAL:

Number of Peer-Reviewed Conference Proceeding publications (other than abstracts):

(d) Manuscripts

Received	Paper

TOTAL:

Number of Manuscripts:

Books

Received Book

TOTAL:

Received Book Chapter

TOTAL:

Patents Submitted

Patents Awarded

Awards

1. PI Renu Tripathi, Panel member on 'Increasing Diversity and Inclusion in Sciences & Engineering', at SPIE Optics + Photonics Conference, San Diego, Aug. 2016

2. PI Renu Tripathi received AAAS award to participate in the AAAS-NSF delegation to Mexico City, April 2016

Graduate Students

NAME	PERCENT_SUPPORTED	DISCIPLINE
Zachary Warren	0	Other (Please Specify); Optics
FTE Equivalent:	**0.00**	
Total Number:	**1**	

Names of Post Doctorates

NAME	PERCENT_SUPPORTED
FTE Equivalent:	
Total Number:	

Names of Faculty Supported

NAME	PERCENT_SUPPORTED	National Academy Member
Renu Tripathi	0.00	
Gour S. Pati	0.00	
FTE Equivalent:	**0.00**	
Total Number:	**2**	

Names of Under Graduate students supported

NAME	PERCENT_SUPPORTED	DISCIPLINE
Kevin Heesh	0	Other (Please Specify): Engineering Phys
Lorna Caesar	0	Other (Please Specify): Engineering Phys
FTE Equivalent:	**0.00**	
Total Number:	**2**	

Student Metrics

This section only applies to graduating undergraduates supported by this agreement in this reporting period

The number of undergraduates funded by this agreement who graduated during this period: 0.00

The number of undergraduates funded by this agreement who graduated during this period with a degree in science, mathematics, engineering, or technology fields:..... 0.00

The number of undergraduates funded by your agreement who graduated during this period and will continue to pursue a graduate or Ph.D. degree in science, mathematics, engineering, or technology fields:..... 0.00

Number of graduating undergraduates who achieved a 3.5 GPA to 4.0 (4.0 max scale):..... 0.00

Number of graduating undergraduates funded by a DoD funded Center of Excellence grant for Education, Research and Engineering:..... 0.00

The number of undergraduates funded by your agreement who graduated during this period and intend to work for the Department of Defense 0.00

The number of undergraduates funded by your agreement who graduated during this period and will receive scholarships or fellowships for further studies in science, mathematics, engineering or technology fields:..... 0.00

Names of Personnel receiving masters degrees

NAME
Total Number:

Names of personnel receiving PHDs

NAME
Total Number:

Names of other research staff

NAME	PERCENT_SUPPORTED
FTE Equivalent:	
Total Number:	

Sub Contractors (DD882)

Inventions (DD882)

Scientific Progress

Technology Transfer

Instrument Development for a Long-Range, High-Resolution 3D Imaging Photon Counting LADAR

DURIP Report (06/15/2015 – 01/14/2017)
Dr. Renu Tripathi
Department of Physics and Engineering
Delaware State University
Dover, DE – 19901

1. Objectives

We proposed to develop a high-resolution three-dimensional imaging LADAR system based on the principle of photon-counting and highly-resolution time-correlated measurements. The photon counting LADAR system was proposed to be designed by acquiring and integrating some of the key components and devices such as picosecond laser sources, single photon detectors, and a high-resolution event timer etc. on a robust optomechanical platform. Imaging capability of the PC-LADAR was also proposed to be enhanced using polarimetric measurements.

2. Accomplishments

Following are some of our notable accomplishments:

- Components for developing the photon counting LADAR (PC-LADAR) system have been acquired. This includes purchasing of major components such as picosecond laser sources (LDH-P-C-705 and LDH-P-C-840, *PicoQuant*), single photon detectors (PD-100-CTC-FC, *Micro Photon Devices* and SPCM-AQRH-16, *Pacer-usa*), picosecond event-timer (HydraHarp 400, *PicoQuant*), and high-bandwidth oscilloscope (DSO-X-4054A, *Keysight Technologies*) etc.
- A software interface for PC-LADAR is developed for performing synchronized beam scanning with the laser transmitter.
- Receiver assembly for PC-LADAR is designed using a large aperture (eight inch) telescope objective lens. Assembly design for the complete system is currently under progress.
- Basic characterizations of the event-timer module for time-of-flight (TOF) measurements have been performed.
- Experiments using a scanning LADAR prototype were conducted to demonstrate improvement in TOF (or range) resolution using a new multi-pulse detection scheme.
- Students (one graduate student and two undergraduate students) are trained in performing LADAR system design, hardware testing and data acquisition.

3. PC-LADAR Development

The PC-LADAR development consists of following steps: a) laser divergence and beam profile characterizations, b) laser beam scanning and transmitter design, c) receiver assembly design, d) performance studies of single-photon detectors, e) testing of event-timer (or time-correlated single photon counting module) in time-of-flight measurements, and finally, f) the LADAR assembly design. Fig. 1a shows the proposed optomechanical layout of the PC-LADAR. The picture in fig. 1b shows an early stage layout of the LADAR being assembled in the lab on an

anodized optical breadboard of dimension (60cm x 60cm x 2.5cm). The complete assembly design and full-scale integration of the PC-LADAR are currently under progress. Kinematic mounts and adaptor plates are designed for easier alignment of the optical and electro-optical

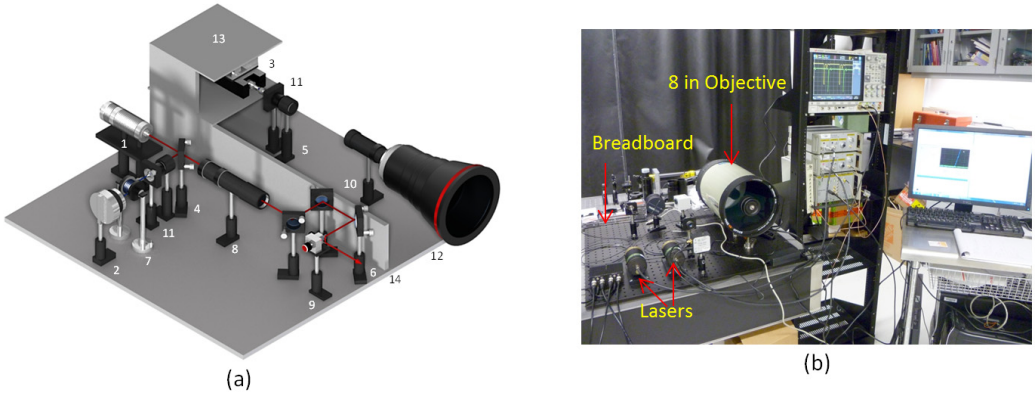

(a) (b)

Fig. 1 Optomechanical layout of the PC-LADAR. Labels: 1. Pulsed laser, 2. 'Start' APD, 3. 'Stop' APD, 4. beam splitter, 5. optical filter, 6. mirror, 7. fiber delay line, 8. beam expander, 9. Beam scanner, 10. relay optics, 11. fiber coupler, 12. objective lens, 13. detector housing, 14. light-shielding partition. (b) an early-stage layout of the LADAR system in the lab.

components such as the scanning mirrors, lenses and detectors used in the system. Lens tube assembly and customized light-shielding partition are used to help minimize unwanted reflections and background light from affecting the daylight PC-LADAR operation. In its final phase, the PC-LADAR instrument will be stationed on a moveable cart for conducting outdoor experiments. In following sections, we discuss experimental development and characterizations of various components and sub-systems that are used in our LADAR instrument development.

3.1 Laser Characterizations

The picture in fig. 1b shows two low-energy ($\simeq$ 0.14 nJ) pulsed laser sources (LDH-P-C-705 and LDH-P-C-840, *PicoQuant*) with wavelengths λ = 705 nm and 840 nm, which are purchased to develop a two-color PC-LADAR system. Both lasers are fiber-coupled diode laser sources featuring easy-to-use controls for laser power levels and repetition frequencies. The driver units (seen in the electronic rack in fig. 1b) for both lasers consist of internal pulse generators that produce low jitter clock signals convenient for the LADAR operation. Alternatively, the laser pulses can also be triggered by sending an external trigger inputs to the driver units. Collimated laser outputs from both lasers are sent to a fast silicon PIN photodiode (TDA 200, PicoQuant) to measure the laser pulse characteristics.

Fig. 2a shows the fast response (sub-nanosecond rise time) of the photodiode to laser pulse for λ = 705 nm, observed using a 500 MHz bandwidth digital oscilloscope (DSO-X 4054A, Keysight Technologies), seen in the electronic rack in fig. 1b. The photodiode gives a negative response. The screen shot from the oscilloscope shows two negative pulses with 100 ns separation corresponding to 10 MHz repetition rate of the laser. The full-width half-maximum (FWHM) of the laser pulse is measured to be approximately 100 ps. We also measured the maximum pulse energy by measuring the average power at a fixed repetition rate of 5 MHz, and found it close to 0.1 nJ which implies a single laser pulse has approximately 500 million photons for conducting LADAR experiments. In practice, the duration of the laser pulse ultimately decides how small of a range (or depth) the LADAR can measure.

Another important characteristic of the LADAR is the divergence angle of the illuminating beam. As the laser beam propagates towards the target, the physical size of the beam increases due to diffraction. The angular divergence (or angular beam width) of the beam can be described

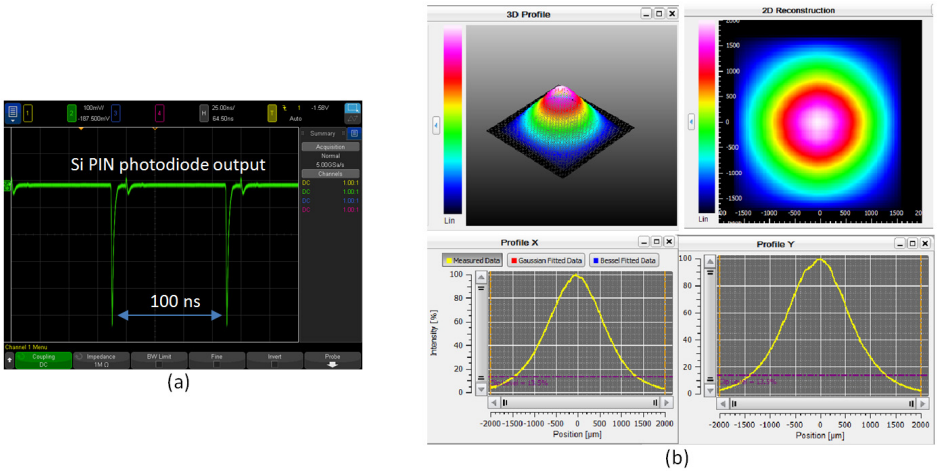

Fig. 2 (a) Response of the PIN photodiode to picosecond laser pulses, and (b) pulsed diode laser beam characteristics measured by the optical beam profiler.

by the expression: $\theta_t = 1.22\,\lambda/D_t$ where D_t is the diameter of the aperture of the transmitting optics. The physical size of the beam at the target decides the spatial (or azimuthal) resolution of the LADAR. The spot size of the beam on the target is given by $\Delta x = \theta_t . R$ where R is the distance to the target. We measured the beam parameters (e.g. beam width and angular divergence) of our pulsed laser systems using an optical beam profiler (BP209, *Thorlabs*). The beam from the pulsed diode laser is collimated using a fiber collimating lens. The pictures shown in fig. 2b show 1D, 2D and 3D beam profiles of the 705 nm diode laser measured using the beam profiler. The beam profiles show close-to-Gaussian beam shapes for the collimated beam with X- and Y-widths close to 3 mm. We also measured the angular divergence θ_t of the laser beam, and found it close to 0.5 mrad which corresponds to a spatial resolution Δx equals to 50 cm at 1 km distance. The spatial resolution can be improved by further expanding the beam at the LADAR transmitter. Similar beam parameters have been measured for our 840 nm pulsed diode laser.

3.2 Beam Scanning: Software Interface Development

The PC-LADAR system development requires scanning of the target pixel-by-pixel in order to illuminate the target with synchronized laser pulses, and then collecting the returning light from the target to obtain range and intensity information. A two-axis galvanometric scanner (shown in fig. 3a) has been used for this purpose. The picture in fig. 3a also shows the controllers that are used to drive the two mirrors in the scanner. One mirror is responsible for x-positioning of the laser beam, while the other mirror is responsible for y-positioning of the beam. While working together, the mirrors can steer the beam to scan a specified target surface. The main limiting factor of this technology is the speed at which the electric motors can rotate the mirrors. Currently, the galvo-scanner used in our LADAR system can operate at speed up to about 1 KHz. Fig. 3b shows a compact two-axis MEMS mirror scanner that we have purchased that can operate at higher speed above 1 KHz. We have developed a software interface to control the galvo-scanner in the LADAR system via LabVIEW virtual environment (VI) on the computer.

This program serves three main functions: i). generating synchronized laser pulses, and raster scanning the two-axis galvo-mirror, ii). acquiring data from the TCSPC hardware, and iii). imaging data with Matlab MathScript RT module (fig. 4a).

Our first program function is designed to control the servo-motors for the x- and y-positions of the galvo-mirrors and to create a software trigger for the laser. The LabVIEW program sends two command signals to the galvo driver board each time we wish to change the position of x and y mirrors by a predetermined step size. The driver board accepts step-signals as voltage ranging

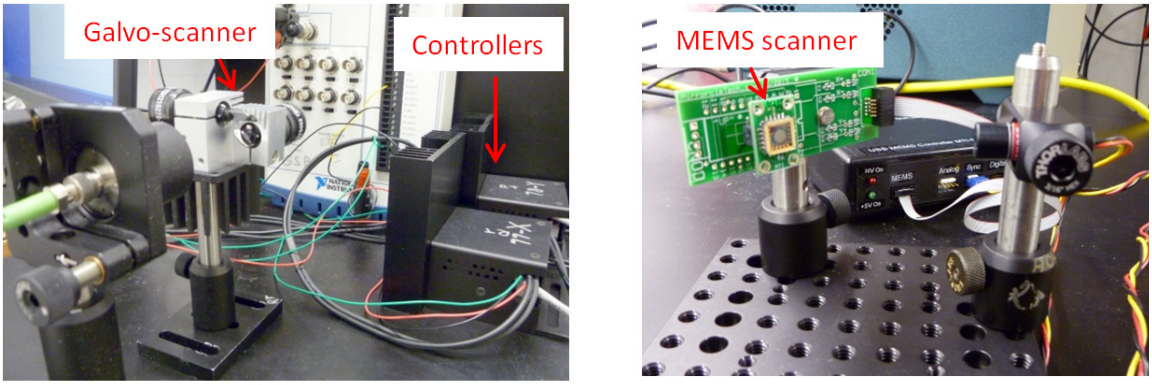

(a) (b)

Fig. 3 Picture showing (a) the two-axis galvanometric scanner which is used in our laser scanning experiments, and (b) a compact two-axis MEMS scanner acquired for our LADAR system development.

from -10 to 10 V, where 1 V corresponds to a 1 degree shift for the corresponding mirror. Maximum angular scanning range for this configuration is 10 degrees. To achieve higher scanning range, the internal jumpers on the driver board could be set to 0.5 V per degree, effectively increasing the field-of-view (FOV) to 12.5 degrees. The x-scan mirror is driven by a saw tooth waveform generator. The amplitude of the saw tooth corresponds to the x-range of the scan in degrees, and the frequency corresponds to scanning speed. During one period of the saw tooth wave, the galvo completes one full row scan. The y-scan mirror is controlled by using a voltage step function, which resembles a slow-growing saw tooth wave. After completion of each x-scan row, the y-scan mirror moves down by one step. The scanning y- range and y- step sizes are set independently through the LabVIEW VI.

First, we developed the interface by triggering the laser with an external waveform generator which produces a 5 V square wave signal of a specified frequency. The function generator triggering the laser was synchronized with the x-mirror generator by the system clock. These two waveforms sharing the same start trigger have constant relative frequency, and, phase relationship. However, we observed that the image in LADAR acquisition is shifted and distorted while increasing the speed of scanning and data acquisition. The key to resolving this issue is that the galvo-mirrors and the laser should be triggered from one source, and remain synchronized during the whole scan. Next, we used the software trigger to trigger the laser by sending a square wave output through a DAQ board. In this case, the galvo-mirror driving code consisted of two DAQ assistants, and LabVIEW functions for sending signals into the DAQ board for x-mirror and y-mirror. The x-mirror control code was placed in a timed loop, the iteration timing of which controls the stepping speed of x-mirror. The y-mirror stepping speed

was controlled with a simple logic code which incremented the voltage and moved the y-mirror after a certain number of x-steps.

The problem with the above approach was that there was no feedback between the start of the software trigger of the laser and the start of the galvo-mirror driving code. However, the two sections of code were in the same virtual environment (VI) and were supposed to start simultaneously, but if one section executed faster than the other, they went out of synchronization leading to the shifted and distorted LADAR images. We quickly realized that this kind of basic synchronization is not good enough for our demanding high-precision timing application. Part of the problem was caused by multiple DAQ assistants used for each DAQ

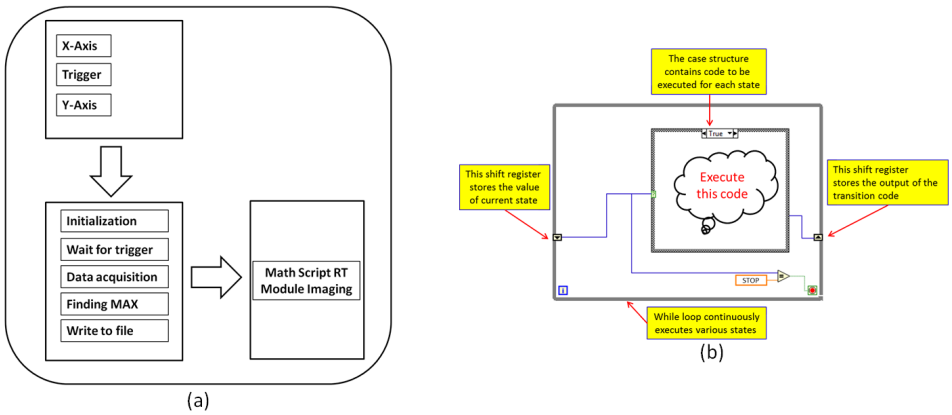

Fig. 4 (a) LabVIEW program operation block diagram, and (b) state machine architecture.

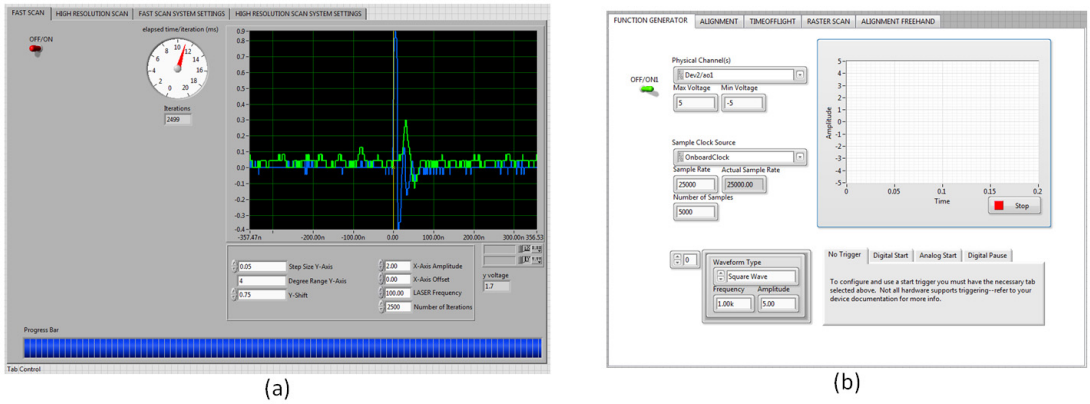

Fig. 5 (a) Front panel of the LabVIEW interface that controls our LADAR system, and (b) front panel which shows the software trigger and the onboard clock being used in performing synchronized laser beam scanning.

board which significantly slowed down the entire code. To overcome these limitations imposed by the predesigned functions (i.e. DAQ assistant), we used NI-DAQmx Application Programming Interface (API) for laser triggering and galvo-mirror driving. Its polymorphic VIs accept multiple data types for same set of functions which solved one of the problems we faced while using predesigned LabVIEW functions.

This API is developed specifically for configuring data acquisition tasks. Synchronization between different devices and functions can be done more efficiently since the clock signals are automatically routed between different functions and devices. In order to implement the DAQmx API for our application, our code was rewritten to change the nested timed loop structure to the state machine architecture. The state machine consists of a while loop with a nested case structure as shown below in fig. 4b. The state machine is used to execute x-mirror scan and y-mirror shift sequentially, thus, triggering the laser continuously while the x-mirror does the scan. The software function generator was also rewritten using the DAQmx API. It was set to generate a square wave signal of fixed 5V amplitude and adjustable frequency, necessary to trigger the laser. The x-mirror driving code is substituted by another software function generator which produced a slow rising saw tooth wave.

During one period of the saw tooth wave, the x-mirror completes one full row scan and the laser generates pulses with a desired frequency. In order for the synchronization to be precise, we created a virtual channel with a common sample clock that takes care of all the essential timings in our system. The end result of this effort is that the laser and the galvo driving function see two signals exactly at the same time with a constant execution speed. The software interface also acquires the LADAR data from the TCSPC hardware. It transfers the specified amount of data from the on-board memory of the digitizer to the Random Access Memory (RAM) of the computer. It initializes the digitizer and configures parameters such as acquisition time, sampling rate, number of samples to acquire and the trigger type. Fig. 5a shows the front panel of the LADAR control developed in the LabVIEW environment. There are two modes available for the scan: fast-scan and high-resolution scan. To make the execution speed of the loop faster, we further optimized our code by taking the digitizer initialization and parameter setup functions outside of the loop. Fig. 5b shows a more detailed picture of the user interface showing the software trigger and the onboard clock being used in performing synchronized laser beam scanning.

3.3 Time-of-Flight Measurements

High-resolution time-of-flight (TOF) measurement is extremely important in PC-LADAR imaging. Fig. 6a shows the picture of our test setup used to measure the TOF resolution. The setup consists of a picosecond laser sources (LDH-P-C-705, PicoQuant) operating at 705 nm wavelength, an optical delay line, a detector, and an event-timer, also known as the time-correlated single photon counting (TCSPC) hardware module (HydraHarp 400, PicoQuant) shown in fig. 6b. A collimated laser beam is generated using a fiber collimator. A periodic train of laser pulses are sent to a delay line situated approximately 1.5 meter away from the collimator as shown in the picture in fig. 6a. The returning laser pulses from the delay line are sent to a detector located adjacent to the collimator. The detector output is sent to the TCSPC hardware module for TOF measurement. The detector used in our experiment is a silicon PIN photodiode (TDA 200, PicoQuant) with an active area of 0.5 mm diameter. It has a peak sensitivity near 800 nm which is ideal for measuring 705 nm laser pulses.

The photodiode gives negative output pulse which is directly coupled to the TCSPC module for TOF measurements. Fast response time of the photodiode is critical to performing an accurate TOF resolution measurement by registering these analog voltage transients in the TCSPC hardware. In the PC-LADAR system, TOF measurement is performed using the photon-counting

detectors. It is important to note that in this case TOF resolution is not limited by the pulse response of the detector, but, rather limited by the timing accuracy of the photon event on the detector. This in practice can be much smaller than the detector's pulse response. Thus, we expect our TOF resolution to improve (by 5 to 10 times) in the actual PC-LADAR system.

The TCSPC module is a critical device for TOF measurement. The module we have acquired (HydraHarp 400: picture shown in fig. 6b) is a programmable TCSPC system, which provides a timing resolution of 1 ps and high measurement rates up to 12.5 million counts per second (Mcps). The device also has large on-board memory to perform real-time histogramming of photon arrival times (or TOFs). Fig. 7a shows the screen shot of the software interface of the TCSPC module using LabVIEW that allows us to display and acquire TOF measurements. As an

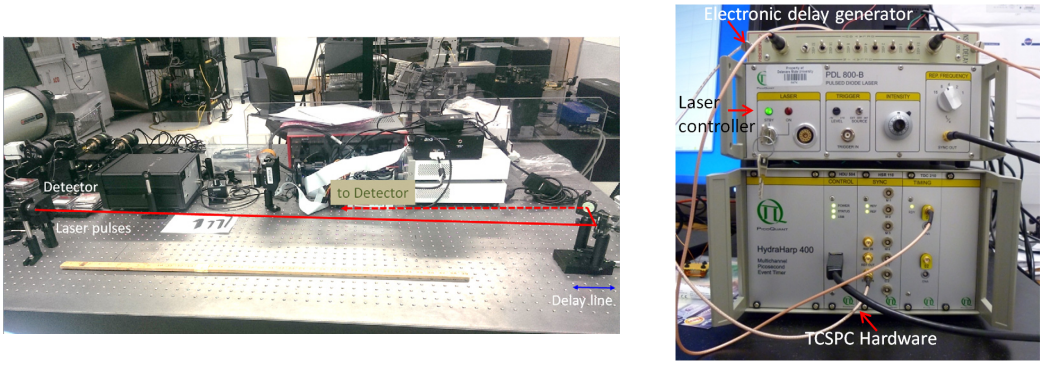

(a) (b)

Fig. 6(a) Picture of the laboratory test setup using a picosecond laser source, optical delay line, APD and TCSPC for measuring TOF resolution for the PC-LADAR system, and (b) picture showing TCSPC hardware along with the picosecond laser controller and the electronic delay generator box.

example, it shows a typical TOF spectrum (or distribution) displayed in the front panel. The horizontal axis in the display corresponds to the number of time bins which can be converted to time delay by considering each individual time bin as 1 ps.

Basic characterizations of the TCSPC module in time delay measurements were initially performed using an electronic delay generator box shown in fig. 6b. In this case, sub-nanosecond electronic pulses were generated by a pulse generator (9520, *Quantum Composer*) which are sent

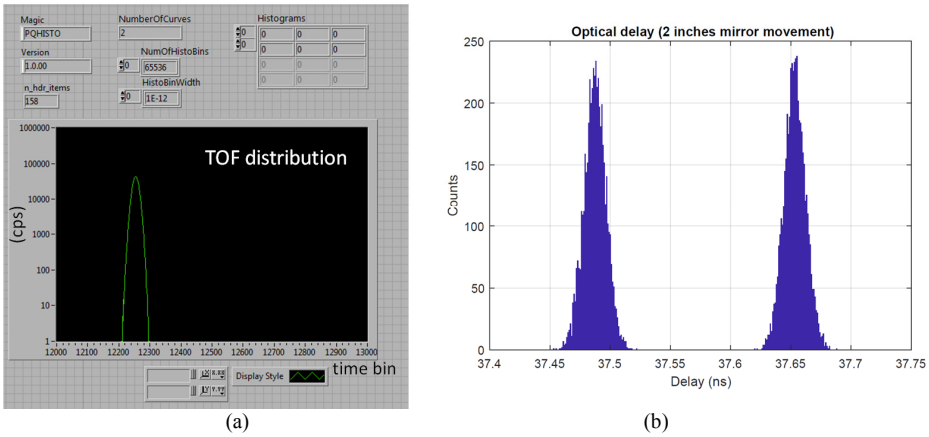

(a) (b)

Fig. 7(a) screen shot showing a LabVIEW front panel of the TCSPC module in operation, and (b) TOF histograms showing two different optical delay measurements.

through the delay generator to create a known delay. This known delay was accurately measured by identifying the peak of the TOF spectrum. The peak in fig. 7a corresponds to an electronic time delay of approximately 12.25 ns. For optical delay measurements, the laser pulses are generated at 5 MHz repetition rate, and the electrical sync output from the laser controller is used as the 'start' timing signal and the photodiode output is used as the 'stop' timing signal for the *TC*SPC module. Although, the round-trip TOF for an individual laser pulse is 10 ns for an optical path of approximately 1.5 meter in our test setup, the time delay observed in the TOF histogram shown in fig. 7b is found to be approximately 37.5 ns. This is caused by an overall electronic delay of the electronic 'stop' pulse with respect to the 'start' timing signal. Fig. 7b shows two TOF histograms which are produced by moving the delay line mirrors by 1 inch away from the detector. The peaks of the histograms are well separated by approximately 170 ps which matched accurately with the optical delay (or path change). We measured the width of TOF histogram which is found to be approximately 50 ps. This suggested that sub-centimeter depth resolution can be achieved by our PC-LADAR imaging.

4. Multi-Pulse Detection Experiments

We have conducted parallel experiments using a new method, known as multi-pulse detection (MPD) technique, for reducing the uncertainty in TOF measurement and improving the range resolution in the scanning LADAR system. Because of different sources of noise associated with the laser pulse, and its detection, amplification and processing, the resolution in measuring TOF (or range) in a scanning LADAR system can often be limited. The timing jitter introduced by these noises mainly determines the precision in TOF or range measurement. In case of long-distance ranging, timing jitter can potentially reduce the range measurement accuracy as the amplitude of laser pulse detected using an analog avalanche photodiode (APD) decreases as the square of the target distance.

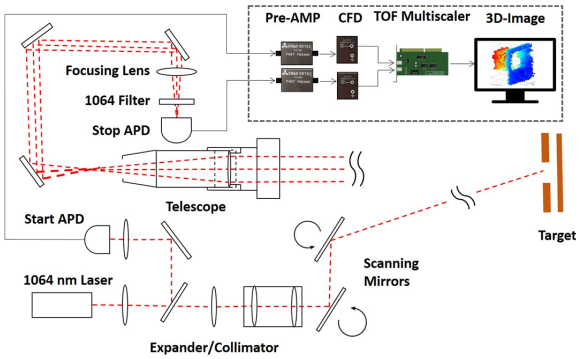

Fig. 8 Schematic of the scanning LADAR prototype designed to implement the MPD technique. (Pre-AMP: pre-amplifier, CFD: constant fraction discriminator)

Fig. 8 shows a prototype scanning LADAR system designed to test the MPD technique. This system is designed by leveraging some components (e.g. beam scanner, analog APD, constant fraction discriminator (CFD), and pulse generators etc.) that we acquired for PC-LADAR design. It employs a Q-switched Nd:YAG laser (1064 nm, pulse duration τ = 9 ns, pulse energy = 1 mJ, and repetition rate = 1 Hz - 1 KHz). A raster beam-scanning has been developed using a pair of (X-Y) galvanometric mirrors (GMs) each having a maximum deflection angle of 12.5 degree. The maximum scan frequency for the X-GM is set to 100 Hz with a minimum stepping angle of 15 µrad. The return light from the target is collected with the 6-inch refracting telescope and focused onto the 0.03 mm aperture of a highly light-sensitive analog APD (rise time = 0.5 ns, gain = 2.5 x 10^4 V/W, NEP = 2 $pW/\sqrt{Hz}$) for TOF (or range) and intensity measurements. Fig. 9 shows the picture of the LADAR prototype along with its components that are enclosed in a

box and mounted on a moving cart for conducting outdoor experiments. The picture in fig. 9b shows the front view of the LADAR transmitter and receiver adjacent to each other.

As mentioned earlier, the transmitter consists of a 1064 nm fiber MOPA laser which is collimated and expanded to produce a 5 mm diameter spot size, and scanned using a two-axis GMs shown in fig. 9e. During experiments, we performed raster scans of the target scene by specifying the step size and the dimensions of the scan. A large aperture 150 mm telescope (Celestron Omni XLT 150, fig. 9b) is used in the LADAR receiver to collect the reflected/back-scattered light signal from the target. The eyepiece of the telescope was removed to allow for a straight view of the image plane. The receiving end of the imaging system was setup as a '4f' optical system as shown in fig. 9(j). After the light was focused at the focal plane of the telescope (or objective lens), a 2 inch diameter bi-convex lens (or focusing lens) of focal length of 75 mm was placed in a way to relay the focal plane onto the APD aperture. This optical configuration ensured collection of maximum amount of light reflected from the target during the scanning LADAR operation. The receiver arm of the LADAR system was separated from the transmitting arm using opaque partitioning dividers and was enclosed in an opaque plastic case in order to avoid unwanted background signals from entering the system.

As shown in fig. 8, a small fraction of the incident beam is reflected to a 'start' APD (APD 310, *Menlo Systems*) which is used as an optical trigger to initiate TOF and intensity measurements from the return signal received by the 'stop' APD. During beam-scanning, the dwell time (i.e. the time spent on illuminating each pixel at the target using the laser pulse) is adjusted through our software control from single-pulse illumination to multi-pulse illumination. The signals received from both 'start' and 'stop' APDs are amplified and fractionally discriminated using the CFDs and the TOF is measured using an electronic multiscaler board (time bin width = 100 ps, bandwidth = 10 GHz). Signal received from the 'stop' APD is also split (not shown in the fig.

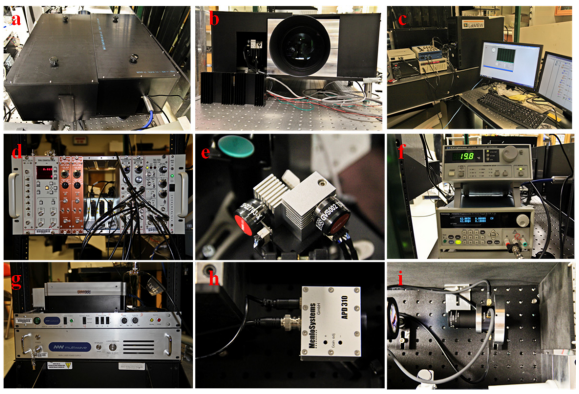

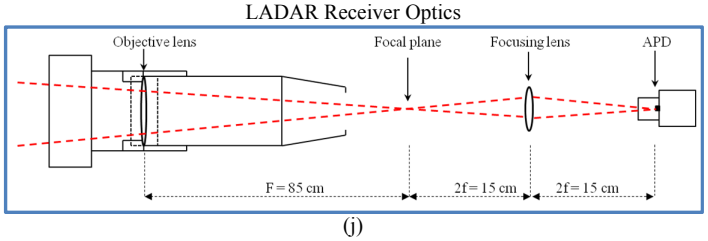

(j)

Fig. 9 **a**. Scanning LADAR prototype enclosed in the box; **b**. front view of the LADAR prototype; **c**. LADAR interface and software control; **d**. time-to-amplitude converter (TAC), two CFDs and a delay generator; **e**. two-axis scanning GM system; **f**. TEC controller and DC power supply; **g**. MOPA fiber laser; **h**. 'start' APD; **i**. 'stop' APD; **j.** receiving arm optics *(drawn not to scale)*.

8), electronically pre-processed and digitized using a fast digitizer board (bandwidth = 300 MHz, sampling rate = 2 GHz/s, PCI 5152, *National Instruments*) to simultaneously obtain the intensity information of the target. Electronic filters are used to reduce high-frequency intensity fluctuations of the signal resulting from our laser instabilities.

To test the operation of the LADAR prototype, we performed range and intensity imaging of several distant targets. The system was operated in two different modes: fast-scanning and high-resolution scanning modes. In a fast-scanning mode, the LADAR system finished a full scan of the scene in 30 seconds producing a (60 × 60) pixel image. In a high-resolution scanning mode, the system finished scanning the scene in 60 second producing a (90 × 90) pixel image. Fig. 10a shows the intensity image of a target with 'DSU' print, placed 5 meter away from the LADAR. The contrast between highly reflective white paper surface and the black color printed font is found to be fairly high. One can also decipher the reflection caused from the aluminum post at the bottom of the 'DSU' printed paper. The light dots on the background correspond to the edges of the optical table that are behind the target. Similarly, figures 10(b-d) show color mapped intensity images of other graphics. In all the pictures, the brighter regions correspond to a higher reflectivity surface (i.e. white paper) and the darker regions correspond to a lower reflectivity surface (i.e. black picture).

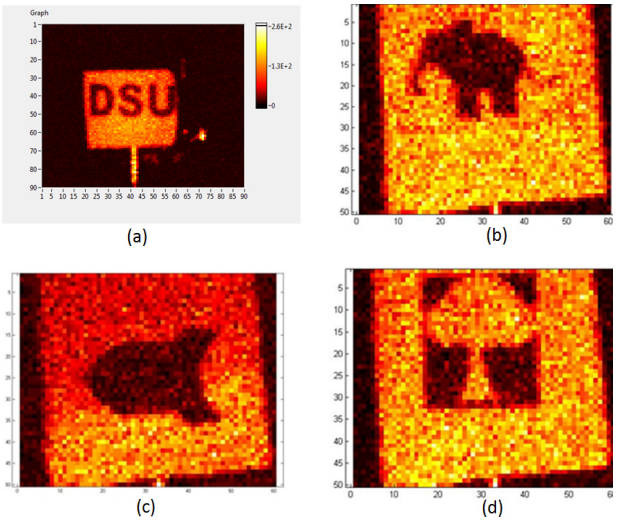

Fig. 10 LADAR intensity images of targets with (a) 'DSU' print, (b) elephant, (c) rocket and (d) tree.

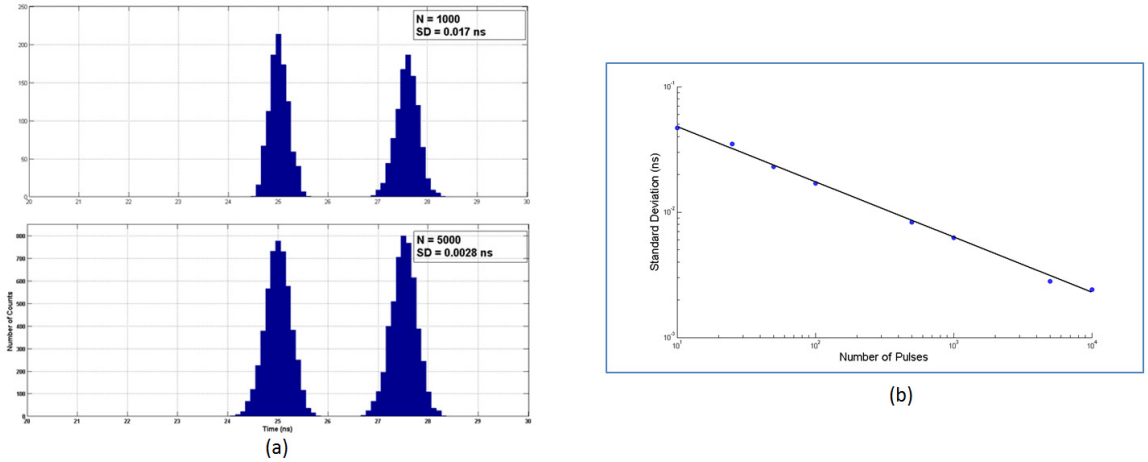

Fig. 11 (a) TOF distributions obtained using multi-pulse illumination for N = 10, 100, 1000, respectively, and (b) plot showing decrease in SNR and normalized standard deviation, solid line – theoretical prediction, dots – experimental measurement.

Typically, in a LADAR system, TOF is measured using a single-pulse detection (SPD) scheme. In this case, each target pixel is illuminated with a single laser pulse, and the single-pulse TOF is obtained by measuring the time interval between 'start' and 'stop' APD signals. Time-to-

amplitude converter (TAC) or time-to-digital converter (TDC) is used as an inexpensive device to measure the time interval between 'start' and 'stop' signals. This device generates a voltage output proportional to the measured time interval. The time resolution of this device is often nonlinear and depends greatly on its full scale range setting. The nonlinearity is caused due to its inherent temperature instability, and differential and integral nonlinearities. Besides these limitations, such a device cannot be easily configured to perform multi-pulse TOF measurement as intended in our experiment.

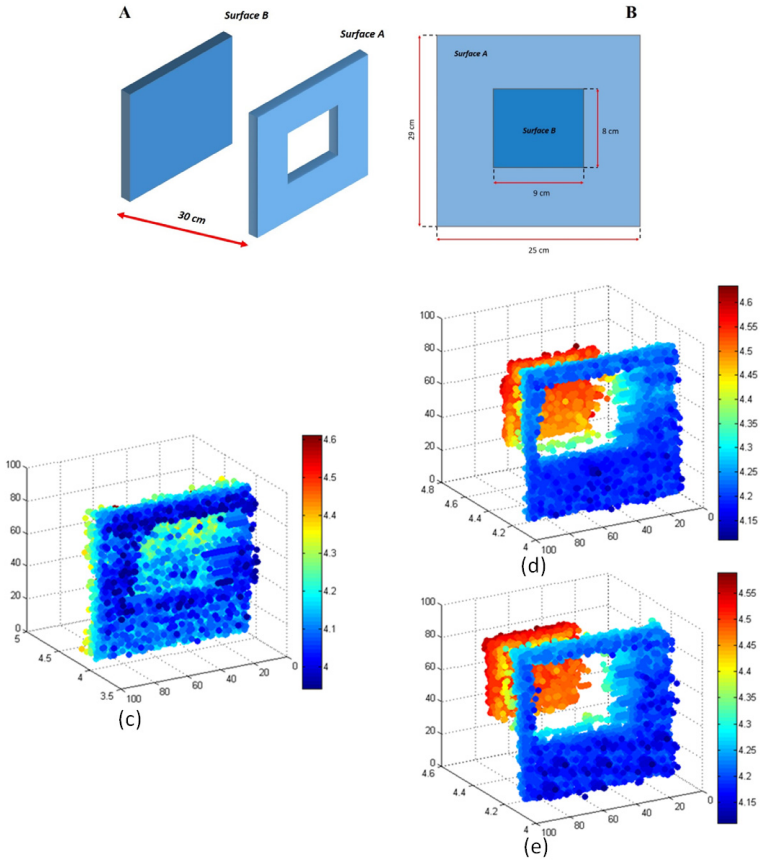

Fig. 12 The 'window' object used in LADAR range imaging: (a) separation between two surfaces, (b) dimensions of the illuminated object surface, and range images (90x90 pixels) of the object surface obtained using multi-pulse detection technique: (c) N = 50 pulses/pixel, (d) N = 100 pulses/pixel, (e) N = 500 pulses/pixel.

The use of the multiscaler board (P7889, *FastComTec*) allowed us to perform multi-pulse detection by measuring the time difference between the signals received from the 'start' and 'stop' APDs corresponding to each laser pulse, and creating a TOF histogram for each target pixel when illuminated by multiple laser pulses. The data is then processed and the peak (or centroid) of the histogram is measured, and the time bin corresponding to the peak (or centroid) of the histogram is used to calculate the TOF and the range for each target pixel. Corresponding pixel intensity information is obtained from the digitizer and is stored. Both TOF and intensity information are combined to form a three-dimensional LADAR image of the target. Although, for demonstration of the MPD technique, a pulsed laser with low repetition rate has been used, in practice, a high repetition rate laser can be used in conjunction with the multiscaler to perform LADAR imaging in real-time (or near real-time).

To test the MPD technique, we initially performed proof-of-principle altimetry measurements without beam-scanning by creating two single-piece targets which were positioned 3.63 m and 4 m away from the LADAR system in our laboratory. These targets were illuminated with a pre-determined number of laser pulses, N and the return signal corresponding to each pulse was acquired by the multiscaler board to create TOF distributions (or histograms) which are shown in fig. 11a. A statistical analysis of the histogram shows a reduction in normalized standard deviation σ_N by a factor 19.5 from N = 10 to 5000. The standard deviation of the histogram determines the resolution in TOF (or range) measurement. This value closely matched the theoretically predicted improvement in standard deviation which is found to be nearly equal to 22 as shown in fig. 11b. The improvement in standard deviation has a $1/\sqrt{N}$ dependence on N illuminating pulses, which confirms the statistical nature of the uncertainty. Thus, our altimetry

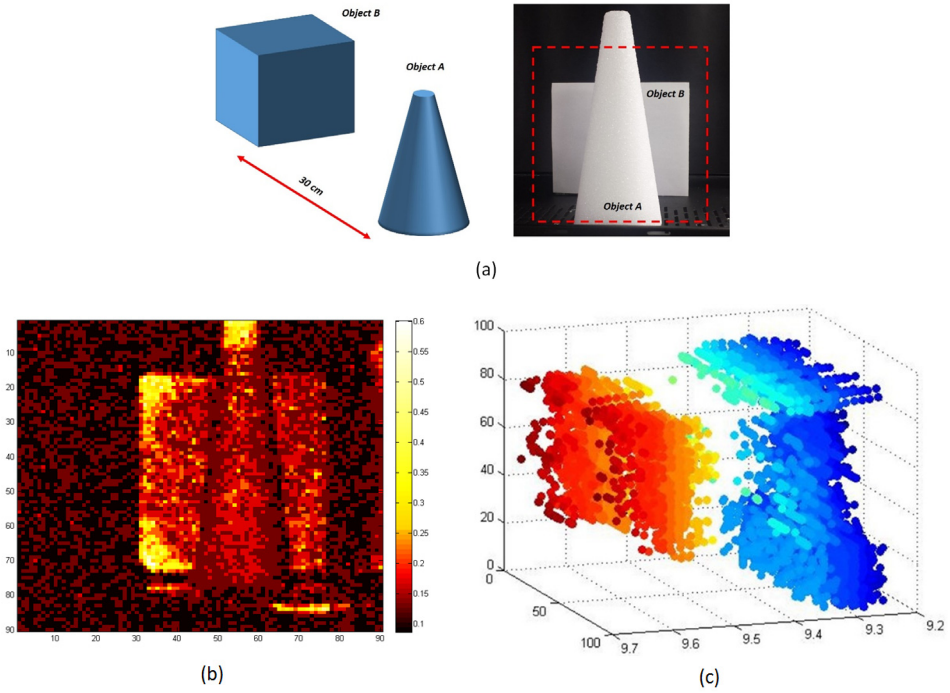

Fig. 13 (a) Cone and cube targets used in long-distance LADAR ranging experiment, (b) intensity image of the target with the color bar showing target reflectivity, and point cloud image of the scene obtained using N = 500 pulses/pixel.

measurements demonstrated that it is possible to reduce the uncertainty in TOF measurement by using the MPD technique. We also found that a continuous increase in N does not lead to a continuous improvement in the TOF resolution, mainly due to the systematic noise present in the system. The primary advantage of MPD is its ability to achieve improved TOF (or range) resolution in the presence of high optical and electronic noise.

To demonstrate improvement in depth resolution in LADAR range imaging with the MPD technique, we performed beam-scanning of a distant object consisting of a cardboard wall with a window and a back wall as shown on figs. 12(a,b). Raster beam-scanning with (90x90) pixels was used to scan and illuminate the object surface with dimension shown in the figure. The range images shown in figs. 12 (c-e) were obtained by illuminating the object with N = 50, 100 and

500 pulses/pixel respectively. The two surfaces of the object shown in fig. 12a are separated by 30 cm.

When the object was illuminated by N = 50 pulses/pixel, the two surfaces cannot be resolved in the range image (fig. 12c) without ambiguity. This is due to the limited resolution in TOF measurement, which was estimated from the histogram to be large (σ = 0.94 ns) for N = 50 pulses/pixel. The standard deviations of TOF histograms were also previously from altimetry measurements to be σ = 0.67 ns for N = 100 pulses/pixel and σ = 0.33 ns for N = 500 pulses/pixel. Based on these observations, it was concluded that MPD range imaging done using N = 500 pulses/pixel should be able to resolve object surfaces with separations as close as 9-10 cm. Range images shown in figs. 12 (d,e) clearly show that both surfaces of the 'window' object are well resolved and their separation distance measured from the range image closely agrees with the actual separation distance (30 cm) between the surfaces.

We also used the scanning LADAR system to test the performance of multi-pulse detection at longer ranging distances. In this case, we set up our experiment in the hallway, and performed both range and intensity imaging using a target with a conical shape (fig. 13). The target consisted of two objects: a cone (10 cm diameter and 20 cm height) and a cube (20 cm edge) made out of Styrofoam. The target was positioned 9.3 m away from the LADAR system. The dotted red square in fig. 13a corresponds to the region which was illuminated during beam scanning to produce (90x90) pixel range and intensity images. Fig. 13b shows the intensity image of the target which was obtained by acquiring the amplitude of the return pulse using the digitizer board. This contains the information about the shape of the target (both objects, the cube and the cone are visible) which can be combined with the range image to achieve better recognition of the target. Fig. 13c shows three-dimensional point cloud range image obtained by illuminating the target with N = 500 pulses/pixel. We can identify the individual target surfaces as well their shapes from the edges. We have also measured the relative locations of the cone and the cube to match closely with their distances from the LADAR system. This shows that multi-pulse detection can provide enhanced range resolution in the LADAR system for field applications.